ADVANCED MATERIALS

Water/Methanol-Soluble Conjugated Copolymer as an Electron-Transport Layer in Polymer Light-Emitting Diodes**

By *Wanli Ma*, *Parameswar K. Iyer*, *Xiong Gong*,* *Bin Liu*, *Daniel Moses*, *Guillermo C. Bazan*,* and *Alan J. Heeger*

The principal criteria for a polymer-based electron-transport layer (ETL) for use in polymer light-emitting diodes (PLEDs) are the following: 1) the lowest unoccupied molecular orbital (LUMO) of the ETL must be at an energy close to, or even within the π*-band of the emissive semiconducting polymer, and 2) the solvent used for casting the electron-injection material must not dissolve the underlying emissive polymer. Although a few attempts to satisfy these criteria have been reported,[1,2] none have succeeded in avoiding interfacial mixing in multilayer PLEDs.

In this contribution, we report the synthesis of the cationic, conjugated alternating copolymer, poly{[9,9-bis(6′-(*N*,*N*,*N*-trimethylammonium)hexyl)-fluorene-2,7-diyl]-*alt*-[2,5-bis(*p*-phenylene)-1,3,4-oxadiazole]} ($PFON^+(CH_3)_3I^-$–PBD), comprising alternating fluorene and phenylene-oxadiazole-phenylene in the main chain, by the palladium-catalyzed Suzuki coupling reaction. Multilayer PLEDs are fabricated using a semiconducting polymer (red-light, green-light, or blue-light emitting; cast from solution in an organic solvent) as an emissive layer and the water-soluble (or methanol-soluble) $PFON^+(CH_3)_3I^-$–PBD as an ETL in the following device configuration: indium tin oxide (ITO)/poly(3,4-ethylenedioxythiophene) (PEDOT)/emissive polymer/ETL/Ba/Al. The results demonstrate that devices with the ETL have significantly lower turn-on voltages, higher brightness, and improved luminous efficiency than those without.

The syntheses of poly{[9,9-bis(6′-(*N*,*N*-dimethylamino)hexyl)-fluorene-2,7-diyl]-*alt*-[2,5-bis(*p*-phenylene)-1,3,4-oxadiazole (polymer **3**),[3,4] and $PFON^+(CH_3)_3I^-$–PBD,[3–6] are shown in Scheme 1. Monomers **1** (0.440 g, 0.654 mmol) and **2** (0.247 g, 0.654 mmol) were dissolved in 20 mL toluene. Sodium carbonate (0.694 g, 6.54 mmol) and $Pd(PPh_3)_4$ (0.037 g, 0.0327 mmol)

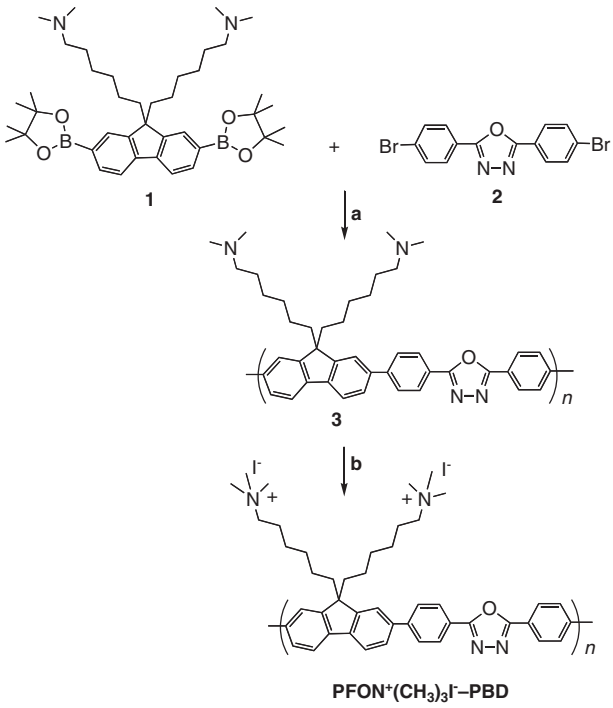

Scheme 1. Synthesis of polymers **3** and $PFON^+(CH_3)_3I^-$–PBD.

were added to the reaction mixture, followed by 5 mL water. The reaction was degassed and refluxed for 48 h under Ar. The reaction mixture was then extracted with chloroform and washed with water and brine. Drying on anhydrous magnesium sulfate, filtration, and evaporation of the solvent gave the crude compound. Precipitating three times from acetone gave the desired polymer **3** (0.231 g, 55 %).

Polymer **3** (0.125 g, 0.195 mmol) was dissolved in 10 mL tetrahydrofuran (THF) and stirred at room temperature, after which 1 mL methyl iodide was added to the reaction. Within 2 min a precipitate formed. After stirring for 30 min, 5 mL water was added to the reaction mixture. Stirring was continued at room temperature for 48 h. The solvent was evaporated to dryness and acetone was added to the flask. The acetone was decanted carefully and this was repeated three times. The precipitates were filtered and dried to obtain the desired polymer, $PFON^+(CH_3)_3I^-$–PBD (0.155 g, 86 %).

Figure 1 compares the current density, *J*, and brightness, *L*, (versus voltage) characteristics of devices made using poly(9,9-dioctyfluorenyl-2,7-diyl) (PFO), with and without

[*] Dr. X. Gong, Prof. G. C. Bazan, W. Ma, Dr. P. K. Iyer, Dr. B. Liu, Dr. D. Moses, Prof. A. J. Heeger
Institute for Polymers and Organic Solids and
Mitsubishi Chemical Center for Advanced Materials
University of California at Santa Barbara
Santa Barbara, CA 93106 (USA)
E-mail: xgong@physics.ucsb.edu; Bazan@chem.ucsb.edu
Prof. G. C. Bazan
Department of Chemistry and Materials Department
University of California at Santa Barbara
Santa Barbara, CA 93106 (USA)
Prof. A. J. Heeger
Department of Physics and Materials Department
University of California at Santa Barbara
Santa Barbara, CA 93106 (USA)

[**] This work was jointly supported by the Mitsubishi Chemical Center for Advanced Materials, the Air Force Office of Scientific Research through the University of Washington MURI Center ("Polymeric Smart Skins"), Program Officer, Dr. Charles Lee, and Dupont Displays (SB030014).

  DOI: 10.1002/adma.200400963

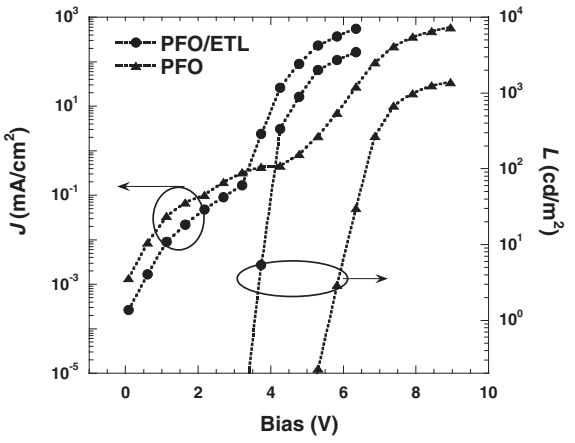

Figure 1. *J* and *L* versus applied voltage (bias) for devices made using blue-light-emitting PFO with and without an ETL.

the ETL. The PFO/ETL device turns on at ~3 V (the turn-on voltage is defined as the voltage at a brightness of 0.1 cd m^{-2}), whereas the turn-on voltage is at ~5 V for the PFO device made without the ETL.[7] At 6 V, the luminance (L) obtained from the PFO/ETL device was $L = 3450$ cd m^{-2}, compared to $L = 30$ cd m^{-2} for the device without the ETL.

Similar improvements were observed in the devices made from the green-light- and red-light-emitting conjugated polymers. For an MEH–PPV/ETL devices, $L = 5600$ cd m^{-2} at 5 V compared to $L = 3550$ cd m^{-2} for similar devices fabricated without the ETL. Therefore, the addition of the ETL resulted in lower turn-on voltages and greater brightness of the diodes.

The improvement in brightness resulted from improved electron injection (there is a good match of the LUMO of the ETL to the π*-band of the emissive polymer) and from the hole-blocking capability of the ETL (LUMO energy at –6.24 eV, relative to vacuum). The reduced turn-on voltage resulted from the enhancement of the built-in potential in the metal–semiconductor–metal diodes by the ETL.[8] Therefore, the effective barrier height for electron injection was lowered, leading to more balanced injection of electrons and holes. As a result, the brightness increased, and the turn-on and operating voltages decreased.

In PLEDs, the device efficiency is reduced by cathode quenching since the recombination zone is typically located near the cathode.[9] The addition of the ETL moves the recombination zone away from the cathode and thereby eliminates cathode quenching. In addition, the ETL serves to block the diffusion of metal atoms, such as barium and calcium, and thereby prevents the generation of quenching centers[9] during the cathode deposition process.

Plots of luminous efficiency (LE, cd A^{-1}) versus J for devices with and without ETLs are shown in Figures 2–4. As shown in Figures 2–4, devices with ETLs have higher luminous efficiency, higher power efficiency, and correspondingly higher brightness at a given voltage.

The improvements in LE and power efficiency (PE) can be understood in greater detail by comparing the LUMO energy

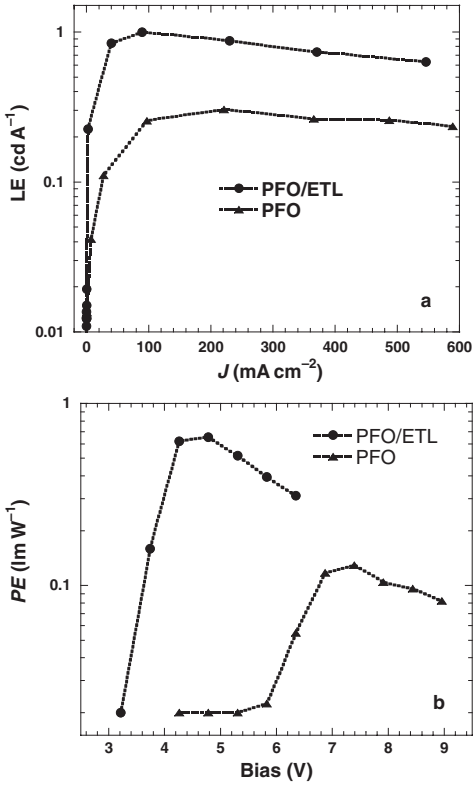

Figure 2. a) *LE* as a function of *J*, and b) power efficiency, *PE*, versus bias for devices made of PFO, with and without an ETL.

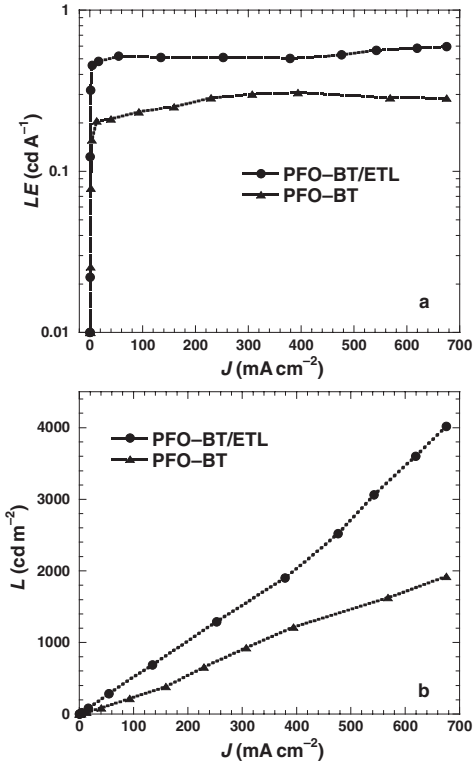

Figure 3. a) *LE* as a function of *J*, and b) *L* versus *J* for devices made of PFO–BT, with and without an ETL.

ADVANCED MATERIALS

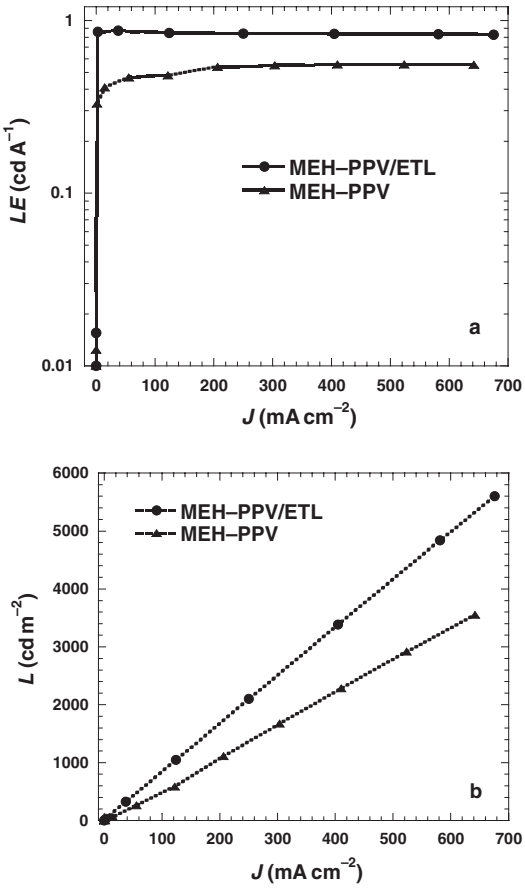

Figure 4. a) *LE* as a function of *J*, and b) *L* versus *J* for devices made of MEH–PPV, with and without an ETL.

levels of the emissive polymers with that of $PFON^+(CH_3)_3I^-$–PBD and the work function of barium (see Scheme 2). The energy barrier between the LUMO of PFO and the work function of barium is ~0.6 eV. Thus, by adding the $PFON^+(CH_3)_3I^-$–PBD layer as the ETL, electron injection is enhanced, resulting in improvements in *LE* and *PE*.

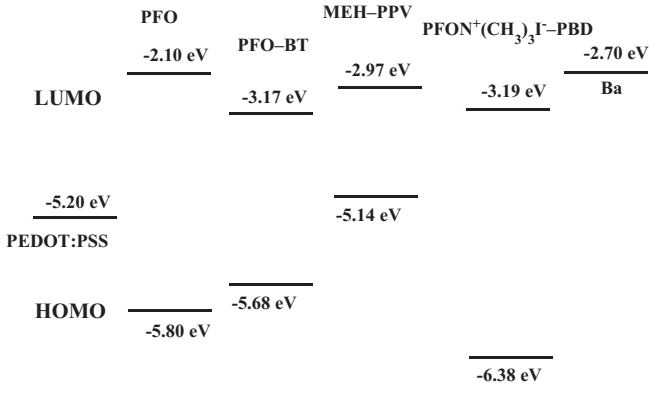

Scheme 2. The HOMO and LUMO energy levels of PFO, PFO–BT, MEH–PPV, and $PFON^+(CH_3)_3I^-$–PBD compared to the work function of Ba (all referenced with respect to vacuum).

For PFO–BT and MEH–PPV, there is no energy barrier for electron injection. However, the hole-blocking feature of the $PFON^+(CH_3)_3I^-$–PBD layer leads to better-balanced electron and hole currents. In addition, the enhanced electron injection can also facilitate hole injection.[10] Therefore, the larger and more nearly balanced electron and hole currents lead to higher luminous efficiencies in the devices with ETLs.

Interfacial energetics are known to play an important role in the emission characteristics of organic LEDs.[11,12] By adding the ETL between the cathode and the emissive polymer, the contacts at both interfaces are improved. Figure 5 shows atomic force microscopy (AFM) images of thin films made

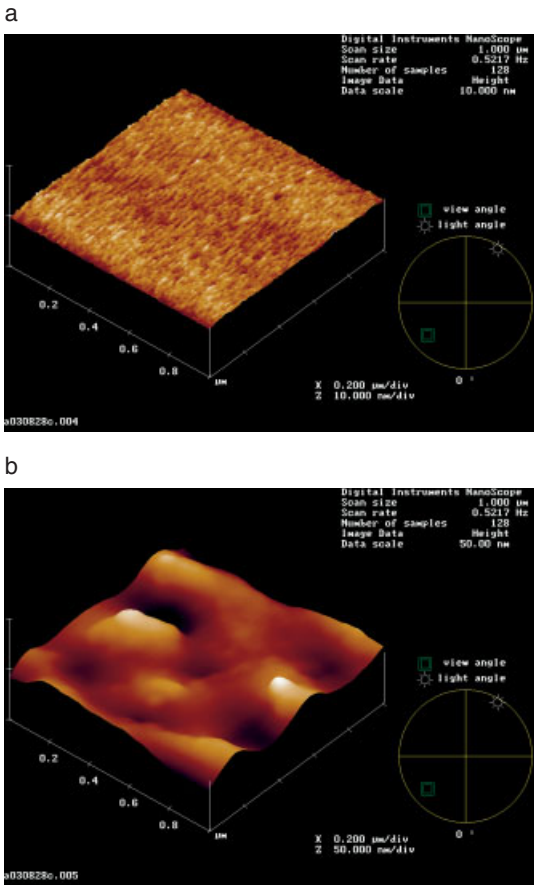

Figure 5. Topographic AFM images of a) PFO and b) $PFON^+(CH_3)_3I^-$–PBD on top of PFO. Both are coated on ITO glass.

from PFO and $PFON^+(CH_3)_3I^-$–PBD on top of PFO. As shown in Figure 5, the surface roughness of the ETL is larger than that of the emissive polymer. As a result, more effective electron injection was achieved simply because of the increased contact area between the ETL and the cathode.

In conclusion, the water-soluble (and methanol-soluble) conjugated co-polymer, $PFON^+(CH_3)_3I^-$–PBD, was designed, synthesized, and utilized as the electron-transport layer in multilayer PLEDs. By casting the ETL from solution in

methanol and the emissive layer from solution in an organic solvent, interfacial mixing was avoided. Using blue-light-, green-light-, or red-light-emitting semiconducting polymers as the emissive layer and PFON$^+$(CH$_3$)$_3$I$^-$–PBD as the ETL, significant improvements in device performance have been demonstrated. Most importantly, our results indicate that high-performance multilayer PLEDs can be fabricated by processing all the layers from solution.

After submitting this manuscript for publication in *Advanced Materials*, Y. Cao and co-workers reported (*J. Am. Chem. Soc.* **2004**, *31*, 9845; *Chem. Mater.* **2004**, *16*, 708) that high external quantum efficiencies were obtained from PLEDs fabricated by water- and/or alcohol-soluble aminoalkyl-substituted polyfluorene copolymers, and that such polymers can be used to fabricate multilayer PLEDs.

Experimental

Characterization of Polymer ***3***: ^{1}H NMR (400 MHz, CDCl$_3$, ppm), δ 8.29 (m, 4H), 7.87 (m, 6H), 7.68 (m, 4H), 2.14 (m, 20H), 1.30 (m, 4H), 1.13 (m, 8H), 0.77 (m, 4H). ^{13}C NMR (125 MHz, CDCl$_3$, ppm) δ 164.76, 152.07, 144.97, 140.91, 139.12, 127.95, 127.62, 126.54, 121.60, 120.67, 59.91, 55.64, 45.57, 40.57, 30.11, 27.70, 27.31, 24.05. Gel-permeation chromatography (GPC) analysis showed a number-average molecular weight of M_n = 19 300 g mol^{-1} and a polydispersity of 1.04.

Characterization of PFON$^+$(CH$_3$)$_3$I$^-$-PBD: ^{1}H NMR (400 MHz, DMSO, ppm): δ 8.30 (m, 4H), 8.07 (m, 6H), 7.88 (m, 4H) 3.13 (m, 4H) 2.94 (m, 22H), 1.43 (m, 4H), 1.06 (m, 8H), 0.61 (m, 4H). ^{13}C NMR (125 MHz, DMSO, ppm) δ 168.94, 151.58, 149.42, 143.62, 137.91, 127.65, 127.62, 126.58, 122.15, 120.98, 65.13, 55.28, 52.05, 42.94, 30.74, 28.710, 25.38, 21.88.

PFO–BT was synthesized using the Suzuki coupling reaction [13,14]. PFO and MEH–PPV were purchased from American Dye Source, Inc. (Canada). The molecular structures of PFO, PFO–BT, and MEH–PPV are shown in Scheme 3. The HOMO (highest occupied molecular orbital) and LUMO energy levels of PFO, PFO–BT, MEH–PPV, and PFON$^+$(CH$_3$)$_3$I$^-$–PBD are shown in Scheme 2. The work functions of PEDOT/poly(styrene sulfonic acid) (PEDOT:PSS) and barium are also shown for comparison in Scheme 2.

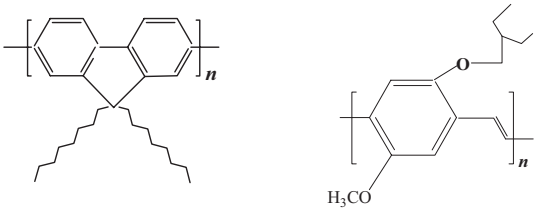

PFO **MEH–PPV**

PFO–BT

Scheme 3. Molecular structures of PFO, PFO–BT, and MEH–PPV.

For device fabrication, we used PEDOT:PSS on ITO as the hole-injecting bilayer electrode. PLEDs were fabricated with and without the ETL layer in the following device structures: ITO/PEDOT:PSS/emissive polymer/Ba/Al and ITO/PEDOT:PSS/emissive polymer/ETL/Ba/Al. The emissive polymers were blue-light-, green-light-, and red-light-emitting conjugated polymers. Details of device fabrication and testing have been reported elsewhere [15,16]; all fabrication steps were carried out inside a controlled atmosphere dry box under a nitrogen atmosphere. The ETL was deposited on top of the emissive layer by spin-casting from a methanol solution (0.6 wt-%) to form a PFON$^+$(CH$_3$)$_3$I$^-$–PBD layer with a thickness of approximately 30 nm, and then annealed at 90 °C for 2 h to remove residual solvent. Hydrophilic methanol was used as the solvent (rather than water) to achieve better interlayer wetting, while maintaining well-defined multilayers.

Received: June 17, 2004
Final version: August 25, 2004

[1] M. Hwang, M. Hua, S. Chen, *Polymer* **1999**, *40*, 3233.
[2] Y. Yang, Q. Pei, *J. Appl. Phys.* **1995**, *77*, 4807.
[3] M. Stork, B. S. Gaylord, A. J. Heeger, G. C. Bazan, *Adv. Mater.* **2002**, *14*, 361.
[4] S. Wang, G. C. Bazan, *Adv. Mater.* **2003**, *15*, 1425.
[5] B. Liu, G. C. Bazan, *J. Am. Chem. Soc.* **2004**, *126*, 1942.
[6] B. Liu, S. Wang, G. C. Bazan, A. Mikhailovsky, *J. Am. Chem. Soc.* **2003**, *125*, 13 306.
[7] M. T. Bernius, M. Inbasekaran, J. O'Brien, W. Wu, *Adv. Mater.* **2000**, *12*, 1737.
[8] Y. Cao, G. Yu, A. J. Heeger, *Adv. Mater.* **1998**, *10*, 917.
[9] V. Choong, Y. Park, Y. Gao, T. Wehrmeister, K. Müllen, B. R. Hsieh, C. W. Tang, *Appl. Phys. Lett.* **1996**, *69*, 1492.
[10] K. Murata, S. Cinà, N. C. Greenham, *Appl. Phys. Lett.* **2001**, *79*, 1193.
[11] J. Cui, Q. Huang, J. G. C. Veinot, H. Yan, T. J. Marks, *Adv. Mater.* **2002**, *14*, 565.
[12] N. C. Greenham, S. C. Moratti, D. D. C. Bradley, R. H. Friend, A. B. Holmes, *Nature* **1993**, *365*, 628.
[13] J. Hunag, Y. H. Niu, W. Yang, Y. Q. Mo, M. Yuan, Y. Cao, *Macromolecules* **2002**, *35*, 6080.
[14] P. Herguth, X. Z. Jiang, M. S. Liu, A. K.-Y. Jen, *Macromolecules* **2002**, *35*, 6094.
[15] X. Gong, J. C. Ostrowski, D. Moses, G. C. Bazan, A. J. Heeger, *Adv. Funct. Mater.* **2003**, *13*, 439.
[16] X. Gong, M. R. Robinson, J. C. Ostrowski, D. Moses, G. C. Bazan, A. J. Heeger, *Adv. Mater.* **2002**, *14*, 581.

